Available online at www.sciencedirect.com
SCIENCE DIRECT®
Journal of Solid State Chemistry 177 (2004) 4569–4575
JOURNAL OF SOLID STATE CHEMISTRY
www.elsevier.com/locate/jssc

Incorporation of rare-earth ions in Mg–Al layered double hydroxides: intercalation with an $[Eu(EDTA)]^-$ chelate

Cang Li, Ge Wang, David G. Evans, Xue Duan*

Key Laboratory of Science and Technology of Controllable Chemical Reactions, Ministry of Education, Beijing University of Chemical Technology, China

Received 18 May 2004; received in revised form 6 September 2004; accepted 12 September 2004
Available online 11 November 2004

Abstract

Reaction of an aqueous slurry of an Mg_2Al–NO_3 layered double hydroxide with a four-fold excess of Na[Eu(EDTA)] gives a material which analyses for $Mg_{0.68}Al_{0.32}(OH)_2[Eu(EDTA)]_{0.10}(CO_3)_{0.11} \cdot 0.66H_2O$. The interlayer spacing of the material is 13.8 Å, corresponding to a gallery height of 9.0 Å, which accords with the maximal dimensions (9–10 Å) of the anion in metal-EDTA complex salts as determined by single crystal X-ray diffraction. Geometrical considerations show that the charge density on the layered double hydroxide layers is too high to be balanced by intercalation of $[Eu(EDTA)]^-$ alone, necessitating the co-intercalation of carbonate ions which have a much higher charge density.

Keywords: Rare earth; Europium; EDTA; Layered double hydroxides; Hydrotalcite

1. Introduction

Rare earths have been the object of considerable scientific and technological interest due to their distinctive optical, electronic, and magnetic properties [1]. Many of them, especially europium and terbium, may be used in luminescent materials (phosphors) because of their sharp and intense emission bands based on *f–f* transitions [2,3]. Complexation of rare-earth ions by organic ligands has been shown to offer considerable advantages in terms of enhanced luminescence efficiency [4]. More recently, europium has attracted wide interest in view of reports [5–8] that persistent luminescent phosphors may be produced by doping Eu^{2+} into alkaline earth aluminates and related oxides. In another area, perovskite-type materials containing rare-earth ions and alkaline earth and/or transition metal ions produced by calcination of mixtures of precursor salts have been shown to have interesting catalytic properties [9,10].

Layered double hydroxides (LDHs), also referred to as hydrotalcite-like compounds or anionic clays, are a family of lamellar solids having the general formula $[M^{II}_{1-x}M^{III}_x(OH)_2](A^{n-})_{x/n} \cdot mH_2O$ [11–13]. Their structure is based on brucite-like layers in which a fraction of the divalent metal cations have been substituted by trivalent cations resulting in positively charged layers. The charge is balanced by intercalation of anions in the interlayer galleries. The value of the stoichiometric coefficient (x) and the identities of the interlayer anions (A^{n-}) and the di- and trivalent intralayer cations may be varied over a wide range. Calcination of LDHs leads [11,14] to formation of mixed oxides whose chemical composition can be easily tuned by adjusting that of the parent LDH. Since the component cations are mixed more uniformly in the LDHs than is possible in a physical mixture, calcination of LDHs may afford superior materials to those produced by calcination of

*Corresponding author. Key Laboratory of Science and Technology of Controllable Chemical Reactions, Directory of Laboratory, Box 98, 15 Beisanhuang Dong Lu, Beijing 100029, China. Fax: +861064425385.
E-mail address: duanx@mail.buct.edu.cn (X. Duan).

0022-4596/$ - see front matter © 2004 Elsevier Inc. All rights reserved.
doi:10.1016/j.jssc.2004.09.005

mixtures of metal oxides. For example, we have shown [15,16] that calcination of LDH precursors containing M^{II}, Fe^{II} and Fe^{III} cations (M^{II} = Mg, Co, Ni) with an M^{2+}: ($Fe^{II}+Fe^{III}$) ratio of 0.5 affords pure ferrite spinels, $M^{II}Fe_2O_4$, which have higher saturation magnetization than samples of the same materials produced by conventional ceramic routes.

LDHs containing rare-earth ions should therefore have potentially interesting properties either in their own right or after calcination to give mixed oxide phases. Although it is generally accepted [11] that the radii of rare-earth cations are too large to be incorporated into brucite-like layers, an alternative route viz. intercalation of anionic rare-earth complexes into the interlayer galleries of LDHs should be feasible. There has been one report [17] in the literature of the uptake of La^{3+} and NO_3^- ions by a nitrilotriacetate-intercalated Mg–Al LDH to form chelate complexes within the layer. Calcination of the resulting material affords a mixture of oxides in which the lanthanum exists as $LaAlO_3$ rather than La_2O_3, indicating that the lanthanum is well dispersed in the oxide matrix and in intimate contact with aluminum. In the case of the closely related EDTA ligand, several groups have recently demonstrated that transition metal-EDTA complexes may be produced by interaction of transition metal cations with an Li–Al LDH pre-intercalated with EDTA [18], by coprecipitation of Mg^{2+} and Al^{3+} in the presence of $[Ni(EDTA)]^{2-}$ [19] and by reaction of calcined LDHs with $[M(EDTA)]^{2-}$ ($M = Fe^{3+}$, Ni^{2+}) which results in reconstruction of the layers with intercalated complex ions [20].

In this paper, we report the synthesis of an LDH material containing Eu^{3+} as its EDTA complex by reaction of an LDH precursor containing interlayer nitrate anions, which are known to be readily displaced by other anions [11]. The logarithms of the stability constants for chelation with Mg^{2+}, Al^{3+}, and Eu^{3+} are 8.64, 16.11, 17.99, respectively [21], indicating that the EuY^- chelate (where Y denotes $EDTA^{4-}$) is more stable than MgY^{2-} and AlY^- and should not therefore give rise to leaching of Mg^{2+} or Al^{3+} cations from the host layers during anion exchange.

2. Experimental

2.1. Reagents

Eu_2O_3 was from Beijing Founder Dongan Rare Earths New Materials Co. Ltd. Other reagents were all of AR grade and obtained from Beijing Yili Fine Chemical Reagent Co. and used without further purification. Deionized water with a conductance below 10^{-6} S cm^{-1} was decarbonated by boiling and bubbling N_2 before use in any synthesis or purification steps.

2.2. Preparation of NaEuY

A mixture of Eu_2O_3 (4.22 g, 0.012 mol) and H_4Y (7.00 g, 0.024 mol) was refluxed in water (300 ml) until the solid had completely dissolved [22]. Aqueous sodium hydroxide solution (1.0 M) was added until the pH reached 6. After concentration and slow evaporation of the solution, a white powder was obtained. The solid was washed with cold water. Elemental analysis: Found% (calc. for $NaEuY \cdot 2.5H_2O$) Eu 29.65 (29.92), Na 4.62 (4.53), C 23.69 (23.62), H 3.54 (3.35), N 5.36 (5.51).

2.3. Synthesis of Mg_2Al–NO_3 LDH

This was prepared by a coprecipitation method. A solution containing $Mg(NO_3)_2 \cdot 6H_2O$ (76.92 g, 0.3 mol) and $Al(NO_3)_3.9H_2O$ (56.27 g, 0.15 mmol) in deionized water (250 ml) was added dropwise to a solution of NaOH (36.00 g, 0.9 mmol) in water (350 ml) under a nitrogen atmosphere [23]. After adjusting the pH to 10, the resulting heavy gel was aged at 65 °C for 39 h. The resulting material was separated by centrifugation and washed with water until the pH of the washings was 7. The solid was stored as a slurry under nitrogen. A small portion was dried at 70 °C for 24 h. Elemental analysis: Found% (calc. for $Mg_{0.69}Al_{0.31}(OH)_2(NO_3)_{0.29}(CO_3)_{0.01} \cdot 0.46H_2O$): Mg 20.06 (19.30), Al 9.99 (9.76), C 0.18 (0.14), H 3.79 (3.40), N 4.94 (4.73).

2.4. Synthesis of Mg_2Al–EUY LDH

A portion of the Mg_2Al–NO_3 LDH slurry (ca. 4.1 g, 3 mmol of dry solid) was added to water (60 ml) and stirred for several minutes. Resulting suspension was added dropwise to a solution of NaEuY. (6.20 g, 12.0 mmol) in water (60 ml). The mixture was stirred for 10 h under N_2 atmosphere at 75 °C. The white solid was separated by filtration, thoroughly washed with hot water and dried at 70 °C for 24 h. Found% (calc. for $Mg_{0.68}Al_{0.32}(OH)_2(EuY)_{0.1}(CO_3)_{0.11} \cdot 0.66H_2O$): Mg 13.70 (13.44); Al 7.08 (7.11); Eu 12.96 (12.49); C 12.15 (10.97); H 4.02 (3.75); N 2.88 (2.31).

2.5. Characterization techniques

X-ray powder diffraction (XRD) data were collected at room temperature on a Shimadzu XRD-6000 powder diffractometer, using following conditions: 40 kV, 30 mA, CuKα_1 radiation ($\lambda = 1.54056$ Å). The samples as unoriented powders, were step-scanned in steps of 5°/min in the range from 3° to 70° using a count time of 4 s per step.

Thermogravimetry and differential thermal analysis (TG-DTA) were carried out under air, with 10 mg of

sample and heating rate of 10.0 °C min^{-1}, using a BOIF instrument (manufactured in Beijing).

Fourier transform infrared (FT-IR) spectra were recorded on a Bruker Vector 22 spectrophotometer. The sample was finely ground for 1 min, combined with oven-dried spectroscopic grade KBr and pressed into a disk. The spectrum of each sample was recorded in triplicate by accumulating 20 scans at 2 cm^{-1} resolution between 400 and 4000 cm^{-1}.

Metal content was determined by ICP emission spectroscopy using an Ultima instrument on solutions prepared by dissolving the samples in concentrated HNO_3. C, H, N content was determined using an Elementarvario elemental analysis instrument.

3. Results and discussion

3.1. Preparation and characterization of Mg_2Al–EUY LDH

Reaction of a suspension of Mg_2Al–NO_3 LDH (which had been stored moist) with a four fold excess of NaEuY for 10 h at 75 °C gives a material which analyses for $Mg_{0.68}Al_{0.32}(OH)_2[EuY]_{0.10}(CO_3)_{0.11}\cdot 0.66H_2O$. The Mg/Al ratio in the product is essentially unchanged from that in the Mg_2Al–NO_3 LDH precursor. Replacement of nitrate ions by EuY^- has been accompanied by co-intercalation of carbonate anions. This phenomenon is often observed, even when attempts are made to exclude atmospheric carbon dioxide, because of the high affinity of the LDH layers for carbonate anions [11]. In this case, the low charge density of the EuY^- anions (vide infra) also favors co-intercalation of carbonate anions.

As shown in Fig. 1, both Mg_2Al–EuY LDH and the nitrate precursor Mg_2Al–NO_3 LDH display the characteristic X-ray powder diffraction patterns of hydrotalcite-like materials similar to those reported in the literature [11,12]. A series of strong (00l) reflections at lower angle and weaker reflections at higher angle are characteristic of layered materials. Intercalation of EuY^- results in an increase in interlayer spacing from 8.7 to 13.8 Å, as shown by the shift of (003) reflection from 10.11° to 6.39°. Furthermore, whereas for the nitrate precursor the intensity of the (003) reflection is greater than that of the (006) reflection, the reverse is true for the EuY intercalate. This is consistent with a considerable increase in electron density in the interlayer region associated with the presence of the Eu^{3+} ions. Given that the thickness of the brucite-like layer of LDHs is 4.8 Å [11], the gallery heights for Mg_2Al–EuY LDH and the precursor Mg_2Al–NO_3 LDH are ca. 9.0 and 3.9 Å, respectively. The gallery height in the former is similar to that observed for FeY^- complexes intercalated in Mg–Al LDHs [20] and MY^{2-} complexes

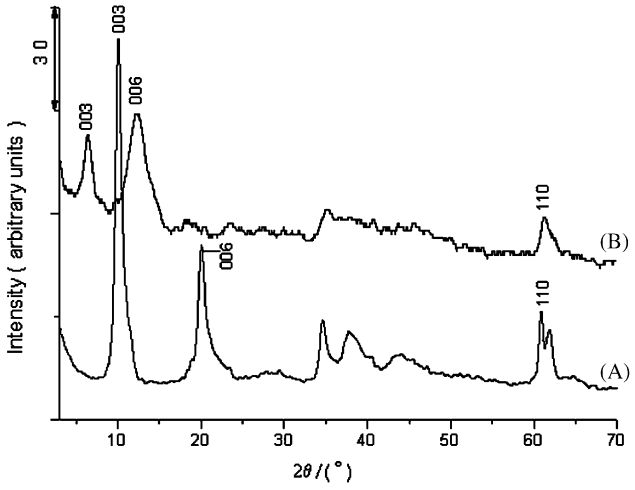

Fig. 1. X-ray powder diffraction patterns of (A) Mg_2Al–NO_3 LDH, (B) Mg_2Al–EuY LDH. Both display the characteristic X-ray powder diffraction patterns of hydrotalcite-like materials with a series of strong (001) reflections at lower angle and weaker reflections at higher angle.

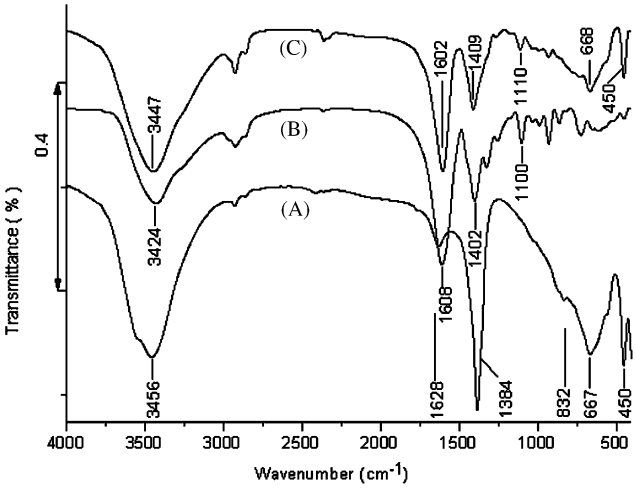

Fig. 2. FT–IR spectra of (A) Mg_2Al–NO_3 LDH, (B) $NaEuY\cdot 3H_2O$, (C) Mg_2Al–EuY LDH. The most intense bands in the spectra of $NaEuY\cdot 3H_2O$, and the EuY-intercalated LDH are the asymmetric and symmetric stretches of the coordinated carboxylate groups at around 1600 and 1400 cm^{-1}, respectively.

(M = Co, Ni, Cu) intercalated in Li–Al LDHs [17] and accords with the maximal dimensions (9–10 Å) of the anion in lanthanide EDTA complex salts as determined by single crystal X-ray diffraction [24].

The FT-IR spectra of the Mg_2Al–NO_3 LDH precursor, NaEuY.$3H_2O$, and the EuY-intercalated LDH are shown in Fig. 2. The spectrum for Mg_2Al–NO_3 LDH is similar to that reported in the literature [25]. The absorption at 1384 cm^{-1} can be assigned to the ν_3 vibration of NO_3^-. A broad strong absorption band

centered at 3456 cm^{-1} is attributed to the stretching vibrations of hydroxyl groups, water molecules in the interlayer, and physically adsorbed water [25]. Both LDHs show bands around 450 and 667 cm^{-1}, which are due to Al–O and Mg–O lattice vibrations [25]. The most intense bands in the spectra of $NaEuY \cdot 3H_2O$, and the EuY-intercalated LDH are the asymmetric and symmetric stretches of the coordinated carboxylate groups at around 1600 and 1400 cm^{-1}, respectively. The wavenumber difference $\Delta v = v_{as} - v_s$ gives information about the coordination environment of the carboxylate group [26]. Unidentate carboxylate groups exhibit Δv values of around 200 cm^{-1} whilst bridging carboxylate groups have Δv values of around 150 cm^{-1}. The values of Δv for $NaEuY \cdot 3H_2O$, and the EuY-intercalated LDH (206 and 193 cm^{-1}, respectively) indicate that the coordination mode of the carboxylate groups is unchanged after intercalation. The slight difference in the value of Δv may be a reflection of the different intermolecular hydrogen bonding environments [26] experienced by the anion in $NaEuY \cdot 3H_2O$ and in the interlayer galleries of the LDH. The intense broad carboxylate symmetric stretching band makes it difficult to confirm the deintercalation of NO_3^- (v_3 expected at 1384 cm^{-1}) and co-intercalation of CO_3^{2-} (v_3 expected at 1365 cm^{-1}) [25] ions suggested above on the basis of the analytical data.

In an attempt to confirm the presence of interlayer CO_3^{2-} ions we recorded the ^{13}C MAS-NMR spectra of $NaEuY \cdot 3H_2O$ and the EuY^- intercalated LDH. In each case a broad peak around 170 ppm is observed for the carbon of the carboxylate groups coordinated to the paramagnetic Eu^{3+} ion, which would obscure any signal from interlayer carbonate ions observed at 174 ppm in LDHs [27]. In a simple qualitative test, addition of dilute HCl to the EuY^- intercalated LDH resulted in considerable effervescence and the evolved gas gave a white suspension with aqueous calcium hydroxide solution ('turned limewater milky'), indicating the presence of CO_2. In contrast, very little gas was evolved when the LDH nitrate precursor was dissolved in dilute HCl. These observations confirm that the EuY^- intercalated LDH contains considerable quantities of carbonate as suggested by elemental analysis.

3.2. Thermal behavior of Mg_2Al–EUY LDH

The features of the thermal decomposition process for LDHs depend on the nature of the layer cations, the nature of the interlayer anions, and the experimental conditions during heating [14,28]. Four steps are generally observed in the thermal evolution of hydrotalcite-like materials: desorption of physically adsorbed water, elimination of the interlayer structural water, dehydroxylation of the brucite-like sheets, and the decomposition of the interlayer anions.

For the nitrate precursor, as shown in Fig. 3A, the first (70–250 °C, 12.2 mass%) weight-loss stage can be assigned to the removal of physically adsorbed and structural water. The corresponding DTA pattern (Fig. 4A) shows a broad endothermic peak (Tm = 148 °C). A major mass loss was observed between 250 and 550 °C (37.7 mass%), resulting from concomitant dehydroxylation of the brucite-like layers and decomposition of intercalated NO_3^- anions.

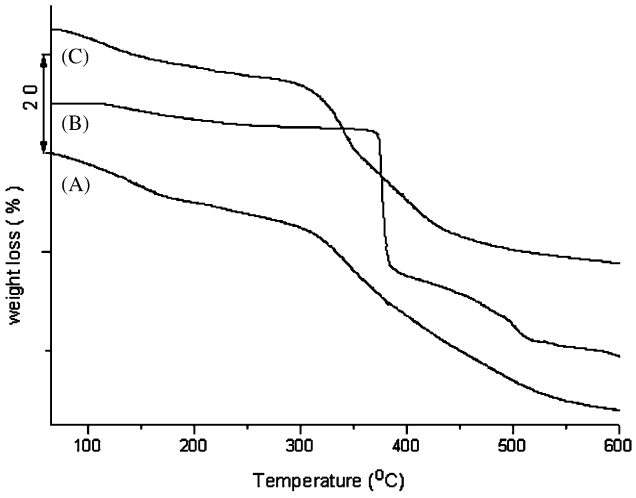

Fig. 3. TG behavior of (A) Mg_2Al–NO_3 LDH, (B) $NaEuY \cdot 3H_2O$, (C) Mg_2Al–EuY LDH. The reduction in mass in C between 70 and 250 °C is due to loss of surface adsorbed and interlayer water. The second event is similar to that of B.

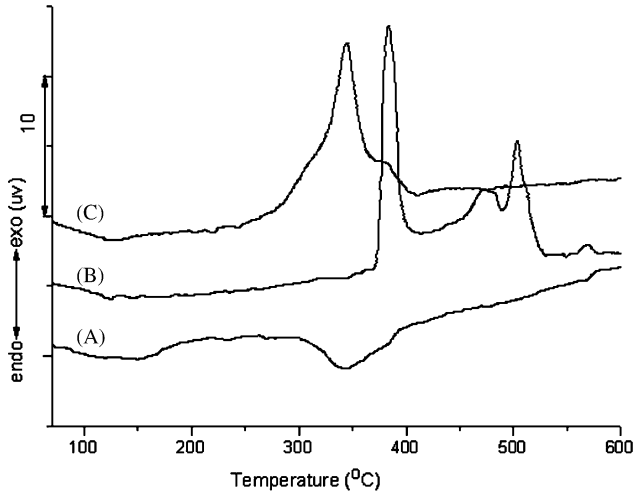

Fig. 4. DTA behavior of (A) Mg_2Al–NO_3LDH, (B) $NaEuY \cdot 3H_2O$, (C) Mg_2Al–EuY LDH. The position of the exothermic peak in the DTA of C is some 40 °C lower than that observed for the B. This may result from the perturbation of the carboxylate groups coordinated to Eu^{3+} induced by interaction with the LDH layers.

The TG curve of the rare-earth chelate complex NaEuY (Fig. 3B) shows four mass loss events. The first one (110–365 °C, 5.3 mass%) corresponds to the elimination of coordinated water. The sharp mass loss observed in the range 365–385 °C (27.9 mass%) is due to combustion of the organic ligand, with a corresponding large exotherm in the DTA curve (Fig. 4B). There is a third mass loss step in the range 385–520 °C (4.9 mass%), with a corresponding weak exotherm in the DTA curve. A similar event in the thermal decomposition of other europium–carboxylate complexes has been ascribed to the formation of the dioxycarbonate $Eu_2O_2CO_3$, accompanied by combustion of small quantities of carbonaceous residues [29] and this may also be the case for NaEuY. The final step (520–620 °C, 4.8 mass%) is associated with the elimination of CO_2, and oxidation of the carbonaceous residue as shown by the small exothermic peak at 570 °C.

The TG trace for Mg_2Al–EuY LDH exhibits three weight-loss events (Fig. 3C). The reduction in mass between 70 and 250 °C (Tm: 126 °C, 9.8 mass%) is due to loss of surface adsorbed and interlayer water (calc. for $Mg_{0.68}Al_{0.32}(OH)_2[EuY]_{0.10}(CO_3)_{0.11}\cdot 0.66H_2O$, 9.7 mass%). The second event (250–360 °C, Tm: 344 °C, 18.0 mass%) is similar to that of the $NaEuY\cdot 3H_2O$ chelate complex. The position of the corresponding exothermic peak in the DTA (Fig. 4C) is some 40 °C lower than that observed for the precursor complex. Typically, the thermal stability of complex anions intercalated in LDHs is higher than that of the free complex [11]. Interestingly, our study shows the reverse result. This may result from the perturbation of the carboxylate groups coordinated to Eu^{3+} induced by interaction with the LDH layers. Alternatively, as demonstrated by single crystal X-ray diffraction [30], the structure of $NaLnY\cdot xH_2O$ complexes consists of a strongly hydrogen-bonded network of hydrated cations and anions which is lost when the complex anions are dispersed in the interlayer galleries and this may be the cause of the greater thermal stability of the precursor complex. Following the decomposition of organic segment is a complex stage (360–550 °C, Tm: 410 °C, 20.6 mass%) involving the combustion of small quantities of carbonaceous residues and dehydroxylation of the brucite-like sheets. The total weight loss below 550 °C is 48.4 mass%, consistent with almost complete decomposition to a mixture of MgO, Al_2O_3 and $EuAlO_3$ (calc. for $Mg_{0.68}Al_{0.32}(OH)_2[EuY]_{0.10}(CO_3)_{0.11}\cdot 0.66H_2O$, 49.7mass%).

Fig. 5A shows the XRD pattern of the LDH after calcination at 1100 °C for 5 h which contains reflections which can be assigned to MgO [31], $MgAl_2O_4$ spinel [32], and $Al_2Eu_4O_9$ [33], as well as weak reflections due to Eu_2O_3, [34]. This indicates that the europium is well dispersed in the Mg–Al oxide matrix. For comparison, calcination of a well-ground mixture of MgO, Al_2O_3 and Eu_2O_3 under the same conditions (Fig. 5B), resulted in a mixture in which only a very small amount of $Al_2Eu_4O_9$ was present.

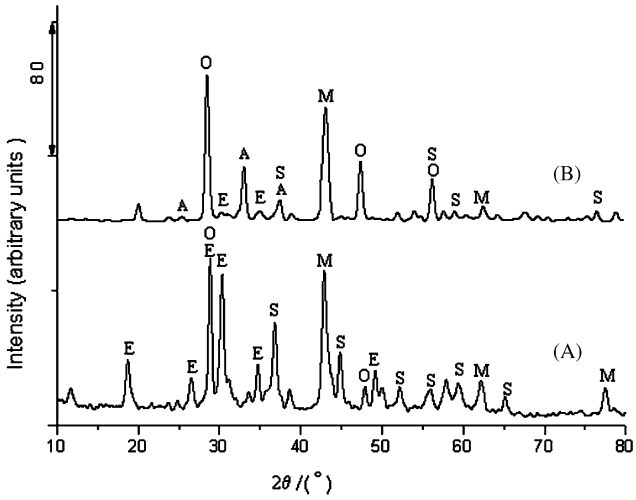

Fig. 5. Powder XRD patterns of (A) Mg_2Al–EuY LDH and (B) a mixture of MgO, Al_2O_3 and Eu_2O_3 after calcination at 1100 °C for 5 h. Reflections are marked for Al_2O_3 (A) [35], MgO (M), $Al_2Eu_4O_9$ (E), $MgAl_2O_4$ (S), Eu_2O_3 (O). The presence of $Al_2Eu_4O_9$ in A indicates that the europium is well dispersed in the Mg–Al oxide matrix.

3.3. Structural model of Mg_2Al–EuY LDH

The structure of LDHs is based on brucite-like layers, where octahedrally coordinated metal ions share edges to form infinite sheets [11]. The area of each $[Mg_{1-x}Al_x(OH)_2]^{x+}$ octahedral unit is related [36] to the unit cell parameter a by the formula: $S=\sqrt{3}(a^2/2)$. The value of a may be estimated from the XRD pattern in Fig. 1B ($a=2d_{110}=3.04$ Å). The area of each octahedral unit is therefore 8.0 Å^2, giving one positive charge per 25 Å^2 for the case of $x=0.32$. As has been noted elsewhere [11], it is this layer high charge density which makes it difficult to exfoliate the LDH layers, in contrast to the behavior of smectite clays. In addition however, the high layer charge density restricts the extent to which anions of low charge density, such as EuY^-, can be incorporated in the interlayer galleries. As discussed above, the gallery height in Mg_2Al–EuY LDH accords with the maximal dimensions (9–10 Å) of the anion in lanthanide EDTA complex salts as determined by single crystal X-ray diffraction [24]. The corresponding cross-sectional area of the complex ions can be estimated to be in the range 65–75 Å^2. Therefore, clearly it is not possible to balance the layer charge by intercalation of EuY^- alone, which explains why co-intercalation of CO_3^{2-} (a small ion with a high charge density) was observed. A schematic representation of the structure of the Mg_2Al–EuY LDH phase is shown in Fig. 6.

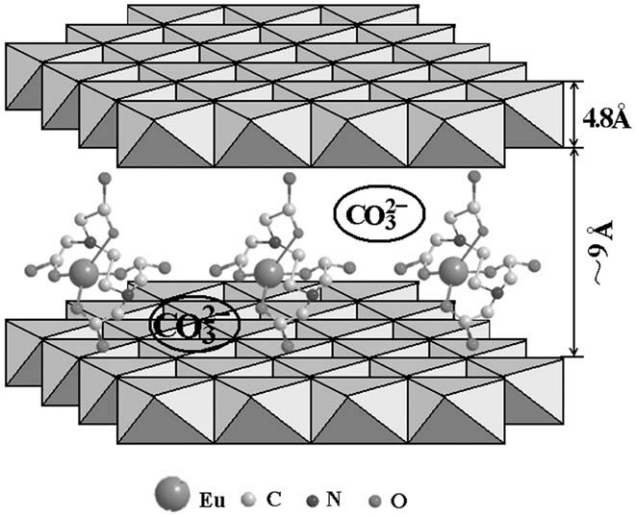

Fig. 6. Schematic illlustration of the possible structure of the EuY^- complex-intercalated LDH. It is not possible to balance the layer charge by intercalation of EuY^- alone, which explains why co-intercalation of CO_3^{2-} was observed.

4. Conclusion

Reaction of an aqueous slurry of an Mg_2Al–NO_3 layered double hydroxide with a four fold excess of NaEuY gives a material which analyses for $Mg_{0.68}Al_{0.32}(OH)_2[EuY]_{0.10}(CO_3)_{0.11} \cdot 0.66H_2O$ containing intercalated EuY^- anions. The interlayer spacing of the material is 13.8 Å, corresponding to a gallery height of 9.0 Å, which accords with the maximum dimensions (9–10 Å) of the anion in metal–EDTA complex salts as determined by single crystal X-ray diffraction. Geometrical considerations show that the charge density on the layered double hydroxide layers is too high to be balanced by intercalation of EuY^- alone, necessitating the co-intercalation of carbonate ions, which have a much higher charge density. After calcination of the LDH at 1100 °C the major europium–containing phase is $Al_2Eu_4O_9$. In contrast, calcination of a mixture of MgO, Al_2O_3 and Eu_2O_3 under the same conditions gave very little $Al_2Eu_4O_9$, with the majority of the Eu^{3+} still present as Eu_2O_3. This indicates that the europium is well dispersed in the LDH and in the resulting Mg–Al oxide matrix after calcination. We are currently investigating the intercalation of other rare-earth complexes in LDHs in order to explore to what extent the degree of rare-earth incorporation can be controlled by tuning the charge density of the precursor complexes.

Acknowledgments

This project was support by the National Nature Science Foundation Of China (No. 90306012) and Beijing Scientific New Star Plan (Grant No. H020821260120).

References

[1] C.R. Ronda, T. Jüstel, H. Nikol, J. Alloys Compd. 275–277 (1998) 669–676.
[2] C. Feldmann, T. Jüstel, C.R. Ronda, P.J. Schmidt, Adv. Funct. Mater. 13 (2003) 511–516.
[3] C. Sanchez, B. Lebeau, F. Chaput, J.-P. Boilot, Adv. Mater. 15 (2003) 1969–1994.
[4] A.-C. Franville, R. Mahiou, D. Zambon, J.-C. Cousseins, Solid State Sci. 3 (2001) 211–222.
[5] T. Aitasalo, P. Deren, J. Hölsä, H. Jungner, J.C. Krupa, M. Lastusaari, J. Legendziewicz, J. Niittykoski, W. Strek, J. Solid State Chem. 171 (2003) 114–122.
[6] J. Hölsä, H. Jungner, M. Lastusaari, J. Niittykoski, J. Alloys Compd. 323–324 (2001) 326–330.
[7] K. Kaiya, N. Takahashi, T. Nakamura, T. Matsuzawa, G.M. Smith, P.C. Riedi, J. Lumin. 87-89 (2000) 1073–1075.
[8] J. Sánchez-Benítez, A. de Andrés, M. Marchal, E. Cordoncillo, M. Vallet Regi, P. Escribano, J. Solid State Chem. 171 (2003) 273–277.
[9] J. Kirchnerova, D. Klvana, Solid State Ionics 123 (1999) 307–317.
[10] D. Weng, H.S. Zhao, X.D. Wu, L.H. Xu, M.Q. Shen, Mater. Sci. Eng. A-Struct. Mater. Prop. Microstruct. Proc. 361 (2003) 173–178.
[11] F. Cavani, F. Trifiro, A. Vaccari, Catal. Today 11 (1991) 173–301.
[12] V. Rives, M.A. Ulibarri, Coord. Chem. Rev. 181 (1999) 61–120.
[13] F. Basile, A. Vaccari, in: V. Rives (Ed.), Layered Double Hydroxides: Present and Future, Nova Science Publishers, New York, 2001 (Chapter 10).
[14] V. Rives, Mater. Chem. Phys. 75 (2002) 19–25.
[15] J. Liu, F. Li, D.G. Evans, X. Duan, Chem. Commun. (2003) 542–543.
[16] F. Li, J. Liu, D.G. Evans, X. Duan, Chem. Mater. 16 (2004) 1597–1602.
[17] M. Kaneyoshi, W. Jones, Mol. Cryst. Liq. Cryst. 356 (2001) 459–468.
[18] K.A. Tarasov, D. O'Hare, V.P. Isupov, Inorg. Chem. 42 (2003) 1919–1927.
[19] A.I. Tsyganok, T. Tsunoda, S. Hamakawa, K. Suzuki, K. Takehira, T. Hayakawa, J. Catal. 213 (2003) 191–203 and references therein.
[20] A.V. Lukashin, A.A. Vertegel, A.A. Eliseev, M.P. Nikiforov, P. Gornert, Yu.D. Tretyakov, J. Nanopart. Res. 5 (2003) 455–464.
[21] J.A. Dean, Lange's Handbook of Chemistry, 15th ed., McGraw-Hill, New York, 1999.
[22] N. Keisuke, T. Kurisaki, H. Wakita, T. Yamaguchi, Acta Crystallogr. C 51 (1995) 1559–1563.
[23] H. Nijs, M. de Bock, E.F. Vansant, Micropor. Mesopor. Mater. 30 (1999) 243–253.
[24] N. Sakagami, Y. Yamada, T. Konno, K. Okamoto, Inorg. Chim. Acta 288 (1999) 7–16.
[25] J.T. Kloprogge, L. Hickey, J.L. Frost, Appl. Clay Sci. 18 (2001) 37–49.
[26] G.B. Deacon, R.J. Phillips, Coord. Chem. Rev. 33 (1980) 227–251.
[27] A. van der Pol, B.L. Mojet, E. van de Ven, E. de Boer, J. Phys. Chem. 98 (1994) 4050–4054.
[28] Z.P. Xu, H.C. Zeng, Chem. Mater. 13 (2001) 4564–4568.

[29] R.N. Marques, C.B. Melios, M. Ionashiro, J. Alloys Compd. 344 (2002) 88–91.
[30] L.R. Nassimbeni, M.R.W. Wright, J.C. van Niekerk, P.A. McCallum, Acta Crystallogr. B 35 (1979) 1341–1345.
[31] JCPDS-ICDD PDF Database 1997 No. 45-0946.
[32] JCPDS-ICDD PDF Database 1997 No. 30-0013.
[33] JCPDS-ICDD PDF Database 1997 No. 03-1162.
[34] JCPDS-ICDD PDF Database 1997 No. 43-1008.
[35] JCPDS-ICDD PDF Database 1997 No. 11-0661.
[36] S.K. Yun, T.J. Pinnavaia, Chem. Mater. 7 (1995) 348–354.